Chalcogenide Letters Vol. 22, No. 7, July 2025, p. 593 - 601

Gamma radiation dose's impact on the energy states and structural properties of $Se_{70}Ge_{20}Sb_{10}$ alloy

J. H. Azzawi [a], Yaseen A. Al-Zahraa [b], M. A. Abdulmajeed [c], K. A. Jasim [c], A. Muravitskaya [e], A. A. Al-Hamadani [d,e], A. H. Al-Dulaimi [d,e]
[a] *Directorate of Education, Diyala, Iraq*
[b] *Ministry of Education, Karkh Education Directorate, Iraq*
[c] *Department of Physics, College of Education for Pure Sciences ibn Al-Haitham, University of Baghdad, Iraq*
[d] *Physics Department, College of Science, University of Diyala, Diyala, Iraq*
[e] *Department of Physics, University of Hull,Hull HU6 7RX, U.K.*

Four $Se_{70}Ge_{20}Sb_{10}$ alloy samples were prepared using the melt quenching technique. To improve the energy states of the mobility gap, the samples were exposed to gamma radiation from 60Co source at various doses of 600, 1200, 1500, and 2000 Gy. The electrical characteristics were examined both before and after irradiation. The conductivity analysis revealed that all of our samples were impacted by gamma radiation. The reorganization of the amorphous lattice and the degree of radiation-induced disorder have been involved in the changes that occurred in the electrical characteristics of the irradiated samples. All irradiated and non-irradiated samples feature three conduction mechanisms at low temperatures, where the electrical conductivity is by hopping electrons between local states close to the Fermi level, according to the identification of the electrical conduction processes. Conduction occurs by transferring electrons between the local levels at the conduction and valence bundles' tails at intermediate temperatures. Conduction occurs in the transfer of electrons between the extended levels in the conduction and valence bands at higher temperatures. It was discovered that all of the local and extended state densities were impacted by the gamma radiation exposure and were computed close to the Fermi level.

(Received April 2, 2025; Accepted July 8, 2025)

Keywords: Melt quenching technique, Mobility gap, Gamma radiation, Hopping of electrons and electrical conductivity

1. Introduction

Amorphous semiconductors based on chalcogenide glasses containing metal atoms offer a compelling platform for advance switching and memory applications due to their tunable electric properties. Their unique structural and electrical properties arise from the presence of chalcogenide like selenium, which forms long chains in glasses [1]. Notably, the addition of metals, such as germanium Ge and selenium Se, characterized by strong covalent bonds and fourfold coordinated germanium, have gathered significant attention for their ease of synthesis, rapid glass formation, and exceptional chemical stability and [2,3].

Extensive research has demonstrated that doping binary systems like Se-Ge with impurity atoms, such as indium, profoundly alters their electrical characteristics [4-6]. The resulting behavior is highly sensitive to glass composition, impurity chemistry, and doping methodology. Importantly, impurity concentration plays a critical role, as not all impurities exhibit electroactive behavior. However, carefully selected impurities can enhance various physical properties, making the study of their effects on chalcogenide glasses vital for both fundamental understanding and practical applications.

Given selenium's significance in electroscopes and the potential to enhance its performance through alloying, researchers have explored binary Se alloys and the incorporation of third elements [7-11]. These additions, including gallium, indium, germanium, arsenic, antimony, bismuth, and tellurium, expand the glass formation region and introduce structural disorder, creating ionic-

*Corresponding authors: kareem.a.j@ihcoedu.uobaghdad.edu.iq
https://doi.org/10.15251/CL.2025.227.593

covalent bonds that increase conductivity in these typically covalent materials. Recent studies have investigated the impact of doping on the density of extended, localized, and Fermi levels, as well as activation energy and tail width, in alloys like $Se_{85}Te_{10}Sn_{5-x}In_x$ [12], $Ge_{30}Te_{70-x}Sb_x$ [13,14], and $Se_6Te4\text{-}xSb_x$ [15]. These investigations highlight the sensitivity of electrical properties to dopant concentration and composition, with observed changes in energy density, electron hopping distance, and other critical parameters [16]. Furthermore, the sensitivity of amorphous chalcogenide semiconductors to ionizing radiation, particularly gamma rays, presents a unique avenue for exploring structural and electronic modifications.[17]

In this study, we aim to elucidate the impact of gamma ray irradiation on the DC electrical conductivity of bulk $Se_{70}Ge_{20}Sb_{10}$ samples across varying temperatures. We will analyze the effects of different gamma ray doses on the densities of localized, extended, and Fermi levels, and their influence on the random energy landscape and structural order. By recording I-V characteristics, we will estimate the DC electrical conductivity, activation energy, and conductance constants. Additionally, we will calculate the densities of various energy states to provide a comprehensive understanding of the interplay between gamma irradiation and electrical transport in this material."

2. Experimental details

The five glassy samples of $Se_{70}Ge_{20}Sb_{10}$ were prepared by melt quenching technique. High-purity Ge, Se, and Sb elemental powder (99.999%) was sealed in an ampoule at a vacuum of 10^{-4} Torr after being weighed according to atomic weight ratios. To prevent unexpected selenium evaporation and precipitation on the inner wall of the quartz tube, the ampoule was then heated in two phases. After gradually heating to 500°C for approximately four hours, the furnace temperature was increased to 920°C and maintained at this temperature for ten hours. The furnace temperature rise rate was 5-6°C/min. To achieve the glassy state, the ampoule was rapidly cooled with ice-cooled water. A pestle and mortar were then used to grind the resulting ingot into the sample powder. The powder was pressed using a hydraulic press with a pressure of 7 tons per square cm to obtain tablets with a diameter of one and a half cm and a thickness of 4 mm.

At room temperature and up to 455 K, the I-V measurements were taken on an electric Keithley scale. I-V measurements as a function of temperature were used to calculate electrical conductivity. The samples were exposed to gamma radiation at various doses of 600, 1200, 1500, and 2000 Gy having their electrical conductivity tested again as a function of temperature. For each sample, the activation energies and electrical conduction processes were identified both before and after irradiation.

3. Results details

The $Se_{70}\,Ge_{20}\,Sb_{10}$ alloy's electrical resistance and conductivity were tested before and fter exposure to gamma radiation in the (292-455) K range of temperatures. The relationship between the electrical conductivity $\ln(\sigma)$ and temperature before and after gamma irradiation exposure is depicted in Fig. 1. All samples have exponential growth of the electrical conductivity with temperature increases as semiconductor materials [18, 19]. Non-exposed sample has moderate growth, but samples after irradiation has a greater rise in electrical conductivity as the gamma radiation dose increases. Similar trends were found for other chalcogenide glasses [18–21]. Important to note that after irradiation, the electrical conductivity of the samples remains semi-conductive and varies only in values but not shape of the curves. Gamma irradiation induces structural modifications within the alloys, potentially leading to alterations in their electrical conductivity [22]. Specifically, irradiation can introduce defects and increase atomic mobility, which, in turn, may facilitate charge carrier transport. However, the precise relationship between irradiation-induced structural changes and conductivity is complex and depends on factors such as the material's composition and the irradiation dose. Observed non-linear dependencies of $\ln(\sigma)$ on 1000/T suggest that conduction mechanisms are influenced by structural imperfections, possibly including grain boundary defects arising from incomplete atomic bonding [25]. These imperfections

contribute to the formation of localized states near the Fermi level. At lower temperatures, these localized states can act as trapping centers, hindering charge carrier mobility and thus reducing electrical conductivity. Conversely, at higher temperatures, thermal activation can assist charge carriers in overcoming potential barriers associated with these trapping states, leading to an increase in carrier mobility and conductivity [26]. The interplay between temperature, defect density, and carrier transport is crucial in determining the overall electrical behavior of the irradiated alloys .

Experimental curves were fitted based on the equation (1) [21 ,20]

$$\sigma = \sigma_{01}\, e^{\left(-\frac{E_1}{KT}\right)} + \sigma_{02}\, e^{\left(-\frac{E_2}{KT}\right)} + \sigma_{03}\, e^{\left(-\frac{E_3}{KT}\right)} \quad (1)$$

where T is the absolute temperature, KB is Boltzmann's constant, (ΔE1, ΔE2, ΔE3) is the activation energy of each term, and $(\sigma_{01}, \sigma_{02}, \sigma_{03})$ are the prior pre-exponential factor parameters. The electrical conductivity was measured for each conduction zone (at low, medium, and high temperatures). According to Figure 1, it appears that the conduction curves in the three thermal regions. The curves show that the conduction through thermal activation has three distinct pathways leading to three distinct slopes generated from three activation energies. In the first region from 400 to 453 K (blue area), the electrical conductivity is caused by the flow of electrons inside the extended region. For the second state at medium range of temperatures from 340 to 400 K (yellow area), the electrical conductivity is caused by the movement of electrons between the tails of the energy bundles within the kinetic gap, and the third state represents the low range of temperatures from 295 to 340 K when the level of electrons hopping between local energy levels near Fermi level [24].

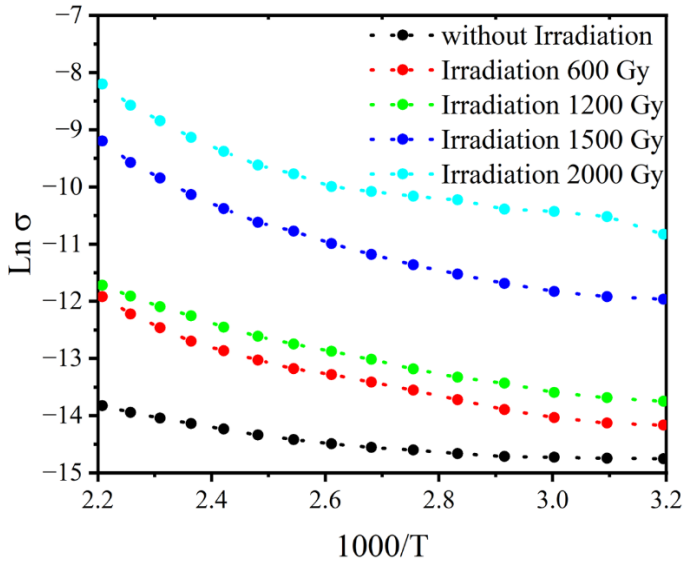

Fig. 1. Ln σ electrical conductivity plot for Se70 Ge20 Sb10 samples as a function of temperature. Colours underline different conduction regimes.

To determine the densities of local and extended states for each sample both before and after irradiation, we extract the activation energies (E_1, E_2, E_3), pre-exponential factor parameters (σ_{01}, σ_{02}, σ_{03}), and the width of the tails ($\Delta E = E_2 - E_1$) from the curves. According to equation 1, the activation energies (E_1, E_2, E_3) can be calculated from the slope of the plot of $\ln(\sigma)$ against 1000/T [24]. The span of the curves and their intersection with the y-axis can be used to compute the pre-exponential factor σ_{01}, σ_{02} and σ_{03}. These values are displayed in Table 1

Table 1. Activation energies (ΔE1, ΔE2, ΔE3) and values of σ01, σ02 and σ03 of $Se_{70}Ge_{20}Sb_{10}$ glasses before and after irradiation..

Radiation Dose	ΔE_1	$\sigma_{o\ extended}$	ΔE_2	$\sigma_{o\ Loc}$	ΔE_3	$\sigma_{o\ fermi}$
0	0.26	6.5	0.078	$5.5*10^{-2}$	$0.5*10^{-2}$	$4.7*10^{-4}$
600	0.33	14.8	0.17	$4.6*10^{-2}$	$5.9*10^{-2}$	$1.05*10^{-2}$
1200	0.50	16.4	0.22	$1.4*10^{-2}$	$5.4*10^{-2}$	$5.2*10^{-2}$
1500	0.42	18.2	0.16	0.23	$5.3*10^{-2}$	$5.5*10^{-2}$
2000	0.41	22.2	0.13	1.54	$5.0*10^{-2}$	$2.4*10^{-2}$

Figure 2 depicts the relationship between the gamma radiation dose and the energy tail width ΔE values (ΔE = E1- E2). This figure shows that the variation in the breadth of the energy tail values with samples exposed to a gamma radiation dose of 600 Gy dropped from 0.19 to 0.16 eV, indicating that radiation impacted the sample's bore structure Because it causes the rearrangement of atoms as a result of the atoms that make up the alloy absorbing radiation energy.

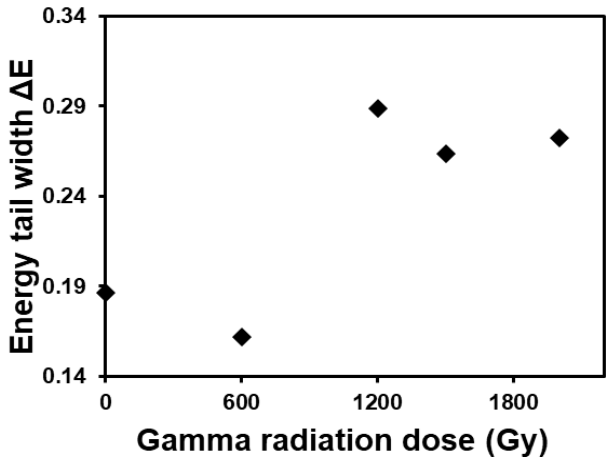

Fig. 2. Films Energy tail width ΔE values plot for $Se_{70}Ge_{20}Sb_{10}$ samples as a function of Gamma Irradiation Dose.

The pre-exponential factor parameters (σ01, σ02, σ03) obtained for all samples were employed to determine the densities of energy states in three localized, extended and Fermi level regions. Using equation 2, we measure the density of extended states.[15]

$$N\ (E_{ext})\ =\ \left[\frac{6m}{e^2\hbar}\right]\sigma_{oext}. \qquad (2)$$

where $N(E_{ext})$=density of extended state, σoext.- conductivity at 0 K, $\hbar = 1.0545 \times 10^{-34}\ J.s$ Table 2 lists the density of extended state values (N(Eext)).The density of extended state increases when gamma radiation dose from $2.12x10^{17}\ eV^{-1}.cm^{-3}\ to\ 9.36x^{21}\ eV^{-1}.cm^{-3}$ at 2000 Gy gamma radiation dose as shown in Figure 3. This is due to a change in activation energy due to gamma irradiation, which may occur for a variety of reasons [12], such as a change in the mobility gap's value, the width of the E tails, the concentration of conductors, or a shift in conductor.[19 ,18]

It can also be observed in this Table how gamma radiation dose affects the density of the localized state which is determined by the equation (3)[18].

$$N\,(E_{loc}) = \left[\frac{6}{e^2 Vph R^2}\right]\sigma_{0loc} \quad (3)$$

where V_{ph} is the phonon frequency, which is of order 1013 s-1and R is the hopping distance and is given $by\ R = 0.7736\left[\frac{\Delta E a^{-1}}{N(E_C)(KT)^2}\right]^{0.25}$ $and\ \gamma^{-1} = 10\,A$. The density of the localized state decreased from $9.54x10^{13}\ (eV^{-1}.cm^{-3})$ at gamma radiation dosage equal to zero to $1.13x10^{10}\ (eV^{-1}.cm^{-3})$ at gamma radiation dose 1500 Gy, then increased to $1.656x^{12}\ (eV^{-1}.cm^{-3})$ when gamma radiation dose reached 2000 Gy, as depicted in Figure 3. According to [27], the change in the density of the extended state and the decrease in the localized state have a significant impact on changing the structure of the alloy from an amorphous to a polycrystalline state.

Because they lack the energy to bridge the grain barrier potential and the conduction includes the grain borders, carriers in polycrystalline materials cannot be transported into the grain by thermionic emission at low temperatures. The disordered atoms and their imperfect bonding produce trapping states, which are dispersed throughout the band gap in the grain boundary trapping model. Some of the trapping states are charged and filled with carriers depending on the temperature as well as on these states are distributed in the gap. When the energy is right, an electron from the charged state might be captured by the empty states. Then, the hopping of charge carriers from filled trap to empty trap states offers an opportunity for conduction. Following the release of the electrons, the filled states might transition into conduction .[28]

To determine the density of the localized state around Fermi level N(EF), we substitute the values for the pre-exponential factor parameters $\sigma 03$ in the low temperatures zone at obtained from Table 1 and compensate them in Equation 4.

$$N\,(E\,F) = \left[\frac{6}{e^2 Vph\,R^2}\right]\,\sigma_{o3} \quad (4)$$

The densities of local states are close to the Fermi level (Figure 3, Table 2). The densities of local states at the Fermi level have often decreased as the gamma dose has increased, indicating that the alloys' structure has changed from random to polycrystalline as a result of the absorption of sample energy radiation [27,28].

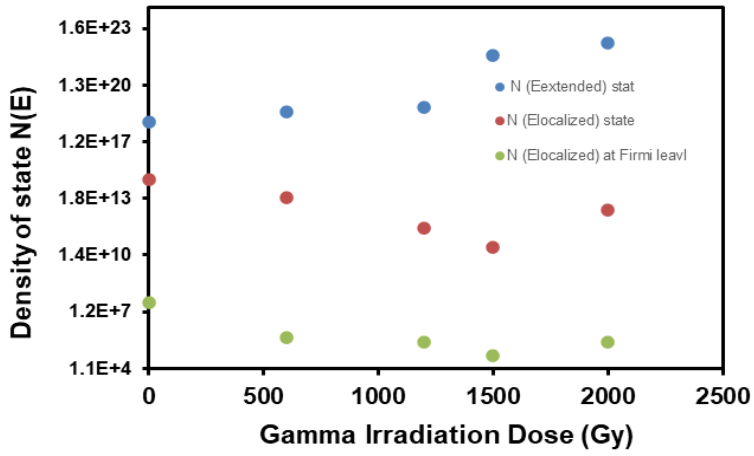

Fig. 3. Densities of energy states in localized, extended and Fermi level regions plot for $Se_{70}Ge_{20}Sb_{10}$.

Figure 4 shows the density of extended state N (Eext), local state N (Eloc.) and at the Fermi N (EF) level as a function of the internal gamma radiation dose. It can be seen from this figure that an increase in gamma radiation causes a decrease in the N (El0c.), N (EF) and an increase in the

density of the extended state N (Eext). The outcomes of the extended, localized, and localized Fermi level density of states at low, medium, and high temperatures. The effect of the gamma radiation on the Se70 Ge20 Sb10 glasses increased the extended state while decreasing the localized states and Fermi level density of states. In Table 2 and Figure 3, it is also mentioned extended energy state densities N (Eext) increased as the Gamma Irradiation Dose increased from 0 to 1500 Ky, while energy state densities in localized N (El0c.) and Fermi level regions N (EF) decreased. However, when the Gamma Irradiation Dose exceeds 1500 Gy, extended, localized, and Fermi-level state densities all increase [29].

Table 2. Tail width ΔE, a, R, N (Ext), N (Eloc) and N(EF) of the ($Se_{70}Ge_{20}Sb_{10}$) alloy are dependent on the dose of gamma radiation.

dose of gamma	tail width (ev)	R A^0	a A^0	N(Ext)	N(Eloc)	N(EF)
0	0.18636	3.743	1.665	2.12E+17	9.54E+13	7.16E+06
600	0.1619	3.743	1.37	9.12E+17	8.73E+12	6.16E+04
1200	0.2886	0.08419	1.27	1.55E+18	1.45E+11	3.70E+04
1500	0.26344	4.30262	1.433	1.83E+21	1.13E+10	5.58E+03
2000	0.2724	0.05519	1.58	9.36E+21	1.656E+12	3.25E+04

3.1. Surface morphology of samples using scanning electron microscopy (SEM)

The surface morphology of samples was studied using a scanning electron microscope (SEM). Figure 4 shows SEM images of the surface of the alloys ($Se_{70}Ge_{20}Sb_{10}$) after exposure to different doses of gamma rays.

The results also showed a clear homogeneity of the samples and the formation of new phases as the compensation for gamma rays plays a role that improves the distribution of the grains and strengthens the cohesion. There is also a decrease in the pores in the microstructure which are considered potential internal defects which indicates the improvement of surface structure.[31]

Scanning electron microscope analysis shown in Figure 4(a, b, c, d and e) showed that the irradiated samples were more uniform compared to the unirradiated sample. The uniformity and clustering of the grains increased as the samples were exposed to radiation. The organization and formation of crystals also depend on the time given to prepare the samples and the duration of their radiation exposure. This was achieved by mixing the components and letting them undergo heat treatment for a while [32, 33].

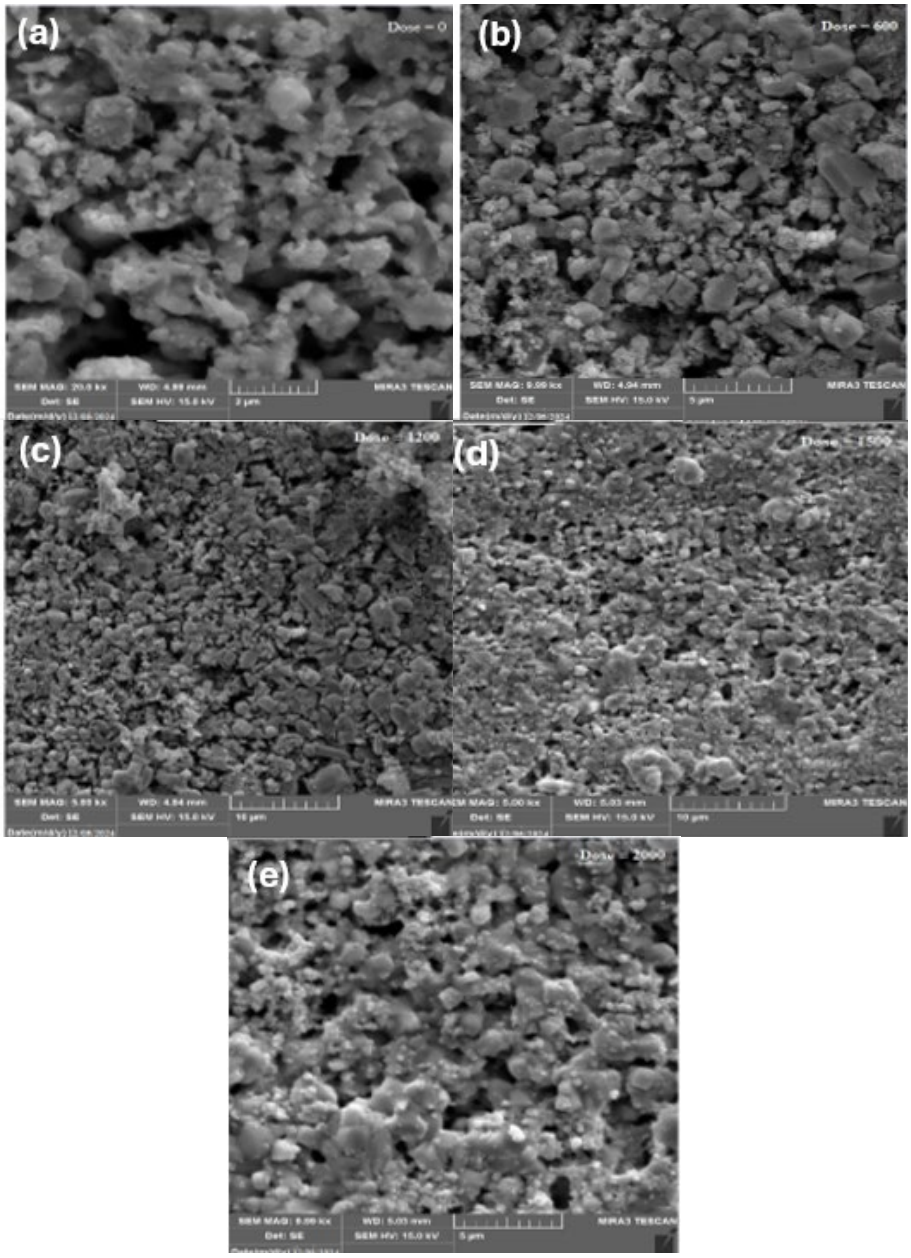

Fig. 4. Scanning electron microscope examination of samples before and after exposure to gamma radiation at different doses of 600, 1200, 1500, and 2000 Gy.

4. Conclusion

This paper, Studies the influence of gamma radiation dose on the density of extended, localized, and localized Fermi level states at low, medium, and high temperatures in the $Se_{70}Ge_{20}Sb_{10}$ alloy produced through the melt quenching process. Three processes of conduction areas were found in the electrical conductivity calculation as a function of temperature, indicating the presence of extended, local, and Fermi-level states. The results also showed a clear homogeneity of the samples and the formation of new phases, where gamma ray compensation plays a role in improving the grain distribution and enhancing cohesion, and the decrease in pores in the microstructure indicates an improvement in the surface structure. The increased homogeneity and clustering of the grains upon exposure of the samples to gamma radiation affected the electrical properties, which is attributed to a change in the density of states (localized extended state density and Fermi level). The densities of the extended energy state (Eext) of the N region (Eloc.) and the N Fermi level (EF)

decreased with increasing gamma radiation dose, affecting the electrical conductivity. When determining the activation energy, it was found that the width of the energy tails changed with the change in gamma radiation dose. The scanning electron microscope (SEM) results showed that the morphologies of the samples were homogeneous and affected by the change in gamma radiation dose.

References

[1] Domínguez, M., Márquez, E., Villares, P., Jiménez-Garay, R. (1995), Physica Status Solidi (a), 147(2), 497-507; https://doi.org/10.1002/pssa.2211470220

[2] Tripathi, S. K., Thakur, A., Singh, G., Sharma, J., Sharma, V., Singh, K. P., Saini, G. S., GoyaL, N. (2005), Journal of Materials Science, 41(6), 1847-1850; https://doi.org/10.1007/s10853-005-3339-z

[3] Tafen, D. N., Drabold, D. A., Mitkova, M. (2005), Physical Review B, 72(5); https://doi.org/10.1103/PhysRevB.72.054206

[4] Kohli, S., Sachdev, V., Mehra, R., Mathur, P. (1998), Physica Status Solidi (B), 209(2), 389-394; https://doi.org/10.1002/(SICI)1521-3951(199810)209:2<389::AID-PSSB389>3.0.CO;2-U

[5] Nagels, P., Tichý, L., Tříska, A., Tichá, H. (1983), Journal of Non-Crystalline Solids, 59-60, 1015-1018; https://doi.org/10.1016/0022-3093(83)90339-3

[6] Tohge, N., Matsuo, H., Minami, T. (1987), Journal of Non-Crystalline Solids, 95-96, 809-816; https://doi.org/10.1016/S0022-3093(87)80685-3

[7] Goel, S., Kumar, A. (1987), Solid State Communications, 64(3), 371-374; https://doi.org/10.1016/0038-1098(87)90985-9

[8] Mohammed, J. S., Nsaif, F. K., Jawad, Y. M., Jasim, K. A., Al Dulaimi, A. H. (2023), Chalcogenide Letters, 20(7), 449-458; https://doi.org/10.15251/CL.2023.207.449

[9] Tripathi, S., Kumar, A. (1988), Journal of Non-Crystalline Solids, 104(2-3), 229-236; https://doi.org/10.1016/0022-3093(88)90393-6

[10] Afifi, M., Hegab, N., Atyia, H., Ismael, M. (2008), Vacuum, 83(2), 326-331; https://doi.org/10.1016/j.vacuum.2008.05.034

[11] Aqeel N. Abdulateef, Ahlam Alsudani, Riyadh Kamil Chillab, Kareem A. Jasim, Auday H. Shaban, Journal of Green Engineering (JGE), 10.9: 5487-5503,2020.

[12] Sharma, N., Sharma, S., Sarin, A., Kumar, R. (2016), Optical Materials, 51, 56-61; https://doi.org/10.1016/j.optmat.2015.11.021

[13] Chillab, R. K., Jahil, S. S., Wadi, K. M., Jasim, K. A., Shaban, A. H. (2021). Key Engineering Materials, 900, 163-171; https://doi.org/10.4028/www.scientific.net/KEM.900.163

[14] Ahmed, B. A., Mohammed, J. S., Fadhil, R. N., Jasim, K. A., Shaban, A. H., Al Dulaimi, A. H. (2022), Chalcogenide Letters, 19(4), 301-308; https://doi.org/10.15251/CL.2022.194.301

[15] Ram, I. S., Kumar, S., Singh, R. K., Singh, P., Singh, K. (2015), AIP Advances, 5(8), 087164; https://doi.org/10.1063/1.4929577

[16] Shpotyuk, O. (1995), Radiation Physics and Chemistry, 46(4-6), 1279-1282; https://doi.org/10.1016/0969-806X(95)00369-9

[17] Khudhair, N. H., Jasim, K. A. (2023), Ibn AL-Haitham Journal For Pure and Applied Sciences, 36(1), 149-157; https://doi.org/10.30526/36.1.2892

[18] Nawal Hassan khudhair, Kareem Ali Jasim, AIP Conf. Proc. 2769, 020062-1-020062-7; https://doi.org/10.1063/5.0129373

[19] Nawal Hassan khudhair, Kareem Ali Jasim, AIP Conf. Proc. 2769, 020056-1-020056-7; https://doi.org/10.1063/5.0129550

[20] Shore, K. A. (2014), Contemporary Physics, 55(4), 337-337; https://doi.org/10.1080/00107514.2014.933254

[21] Jasim, K. A. (2013), Turkish Journal OF Physics; https://doi.org/10.3906/fiz-1203-16

[22] Zainab j. Neamah, Balqees A. Ahmed, Mohammed A. Thejeel, Kareem A. Jasim, Auday H. Shaban, Materials Science Forum, Vol. 1050, pp 41-47, (2022); https://doi.org/10.4028/www.scientific.net/MSF.1050.41

[23] Adler, D. (1975), Science, 188(4184), 141-142; https://doi.org/10.1126/science.188.4184.141.b

[24] Lee, J.., Park, S. D., Kim, B. S., Oh, M. W., Cho, S. H., Min, B. K., Lee, H. W., Kim, M. H. (2010), Electronic Materials Letters, 6(4), 201-207; https://doi.org/10.3365/eml.2010.12.201

[25] Mobarak, M., Shaban, H., Elhady, A. (2008), Materials Chemistry and Physics, 109(2-3), 287-290; https://doi.org/10.1016/j.matchemphys.2007.11.025

[26] Sikka, P., Ferdinand, K. V., Jagadish, C., Mathur, P. C. (1985), Journal of Materials Science, 20(1), 246-254; https://doi.org/10.1007/BF00555918

[27] Paul, D. K., Mitra, S. S. (1973), Physical Review Letters, 31(16), 1000-1003; https://doi.org/10.1103/PhysRevLett.31.1000

[28] Thouless, D. J. (1980), The international series of monographs on physics. Science, 207(4436), 1196-1197; https://doi.org/10.1126/science.207.4436.1196-b

[29] Ibrahim, Z.H., Ibrahim, S.A., Shaban, A.H., Jasim, K.A., Mohammed, M.K., Baghdad - Iraq with Aid of GIS Techniques, Energy Procedia, 2017, 119, pp. 709-717; https://doi.org/10.1016/j.egypro.2017.07.098

[30] Mahdi, S.H., Jassim, W.H., Hamad, I.A., Jasima, K.A., Energy Procedia, 2017, 119, pp. 501-506; https://doi.org/10.1016/j.egypro.2017.07.059

[31] Ho Soonmin, A scanning electron microscopy investigation of semiconductor metal chalcogenide thin films: A review, Der Pharma Chemica, 2016, 8(2):13-16.

[32] Kh. M. Guliyeva, N. N. Mursakulov, N. A. Aliyeva, Y. I. Aliyev, International Journal of Modern Physics BVol. 37, No. 12, 2350116 (2023); https://doi.org/10.1142/S0217979223501163

[33] Y. Handa, T. Suhara, H. Nishihara, J. Koyama, Applied Optics Vol. 18, Issue 2, pp. 248-252 (1979); https://doi.org/10.1364/AO.18.000248